

## Distribution of Sr and Ca Isotopes in Fluids of Lahendong Geothermal Field

Bettina A. Wiegand<sup>1</sup>, Maren Brehme<sup>2</sup>, Yustin Kamah<sup>3</sup> and Martin Sauter<sup>1</sup>

<sup>1</sup>Univ. Göttingen, GZG, Goldschmidtstr. 3, 37077 Göttingen, Germany.

<sup>2</sup>Helmholtz Centre Potsdam – GFZ, Telegrafenberg, 14473 Potsdam, Germany.

<sup>3</sup>Pertamina Geothermal Energy, Jl.M.H. Thamrin No.9, Jakarta 10340, Indonesia.

Email: bwiegan@gwdg.de

**Keywords:** Lahendong geothermal field, Sr isotopes, Ca isotopes

### ABSTRACT

Naturally occurring Sr and Ca isotopes can help to understand geochemical processes like mineral dissolution/precipitation and solute sources in geothermal systems. To test the potential of the two isotope systems, we conducted research in a high-temperature liquid-dominated system located in volcanic rocks in North Sulawesi (Indonesia). Fluids were collected from hot springs, shallow groundwater wells, geothermal production wells, and surface waters in the Lahendong area. The results of the investigations show that the Sr isotope compositions of the fluids vary with the source of solutes and differences in the  $^{87}\text{Sr}/^{86}\text{Sr}$  ratio reflect geochemical differences of andesitic and basaltic rocks in the reservoir and at the surface. In contrast, the distribution of Ca isotopes in the fluids is largely affected by fractionation effects resulting from the precipitation of Ca-bearing mineral phases.

### 1. INTRODUCTION

Sr isotopes have been widely used to decipher sources of solutes in shallow groundwater systems (e.g. Bullen et al., 1996; Wiegand et al., 2001; Wiegand 2009). A number of studies additionally employed Sr isotopes to characterize deep saline fluids in continental settings and geothermal systems (e.g. Elderfield und Greaves, 1981; McNutt et al., 1987; Graham, 1992; Aquilina et al., 1997; Grobe et al., 2000; Grimes et al., 2000; Millot und Négrel, 2007; Millot et al., 2012). Dissolution of minerals by water-rock interaction produces solutes with  $^{87}\text{Sr}/^{86}\text{Sr}$  isotope ratios characteristic for the weathering mineral phases. Therefore, the Sr isotope ratio of thermal water can provide important insights to better understand the genesis of fluids, flow paths, and mixing processes in geothermal systems.

In contrast to the Sr isotope system, Ca isotopes have scarcely been used in groundwater research (e.g. Jacobson and Holmden, 2008; Brown et al., 2013; Druhan et al., 2013), while a number of studies are focused on surface water systems (e.g. Tipper et al., 2008; Wiegand and Schwendenmann, 2013). Unlike the Sr isotope system, which is controlled by radioactive decay of  $^{87}\text{Rb}$  to  $^{87}\text{Sr}$  and therefore the  $^{87}\text{Sr}/^{86}\text{Sr}$  ratio of natural water depends on the age and Rb content of the dissolving mineral phases, variation of Ca isotopes are generated by fractionation processes including precipitation of Ca-bearing mineral phases from aquatic solutions. For example, experimental studies show that Ca isotopes fractionate during precipitation of calcite (e.g. Lemarchand et al., 2004; Tang et al. 2008). Studies of natural hydrological systems have confirmed the experimental results (e.g. Wiegand et al., 2006; Nielsen and DePaolo, 2013). These observations suggest that Sr and Ca isotopes may potentially help to better understand mineral dissolution and precipitation processes, sources of solutes, and groundwater mixing in geothermal systems.

The present study is focused on the geochemical evolution of thermal waters from the high-enthalpy geothermal system of Lahendong in North Sulawesi (Indonesia).  $^{87}\text{Sr}/^{86}\text{Sr}$  ratios and  $\delta^{44}\text{Ca}$  values were investigated to distinguish sources of dissolved Sr and Ca, and elucidate possible interaction between shallow and deep groundwater systems. Samples were collected from hot springs and deep production wells, and compared to data from surface water (lakes, river) and shallow groundwater wells located in the surroundings of the geothermal field.

Lahendong geothermal field is a hot water-dominated system situated within a structurally complex volcanic setting (e.g., Koestono et al., 2010; Utami, 2011; Brehme et al., 2014). Exploration of Lahendong geothermal field began in the 1970s (e.g., Surachman et al., 1987). The current power production capacity is 80 MW (Operator: Pertamina Geothermal Energy). Surface indications for geothermal activity are manifestations including hot springs, mud pools, and gas vents (e.g., Koestono et al., 2010; Utami 2011). Typical reservoir temperatures are 250 °C at about 1000 m below the surface (Utami, 2011). Groundwater in the deep reservoir is characterized by Cl-SO<sub>4</sub>-HCO<sub>3</sub> and Cl-type waters, while HCO<sub>3</sub><sup>-</sup> and SO<sub>4</sub><sup>2-</sup> type waters discharge at the surface (e.g. Utami, 2011; Brehme et al., 2014). Petrological investigations of hydrothermal alterations were conducted by Utami (2011). Koestono et al. (2010) published a first geothermal model of Lahendong, suggesting that intrusion of a diorite complex located beneath Lake Linau provides the heat source of the system.

### 2. GEOLOGICAL SETTING

Lahendong geothermal field is located about 30 km south of the city of Manado and about 10 km west of Mount Tondano (Fig. 1). It is situated in the large volcano-tectonic depression of the Tondano caldera, surrounded by active strato-volcanoes including the Lokon and Mahawu to the north, and the Soputan to the south, while the caldera rim of the ancient Tondano volcano including Lake Tondano form the eastern boundary (Surachman et al., 1987). Elevations in the Lahendong area are between 600 m and 900 m above sea level. Drainage of the area is mainly to the west, where the volcanic structure of the Tondano caldera is open (Surachman et al., 1987).

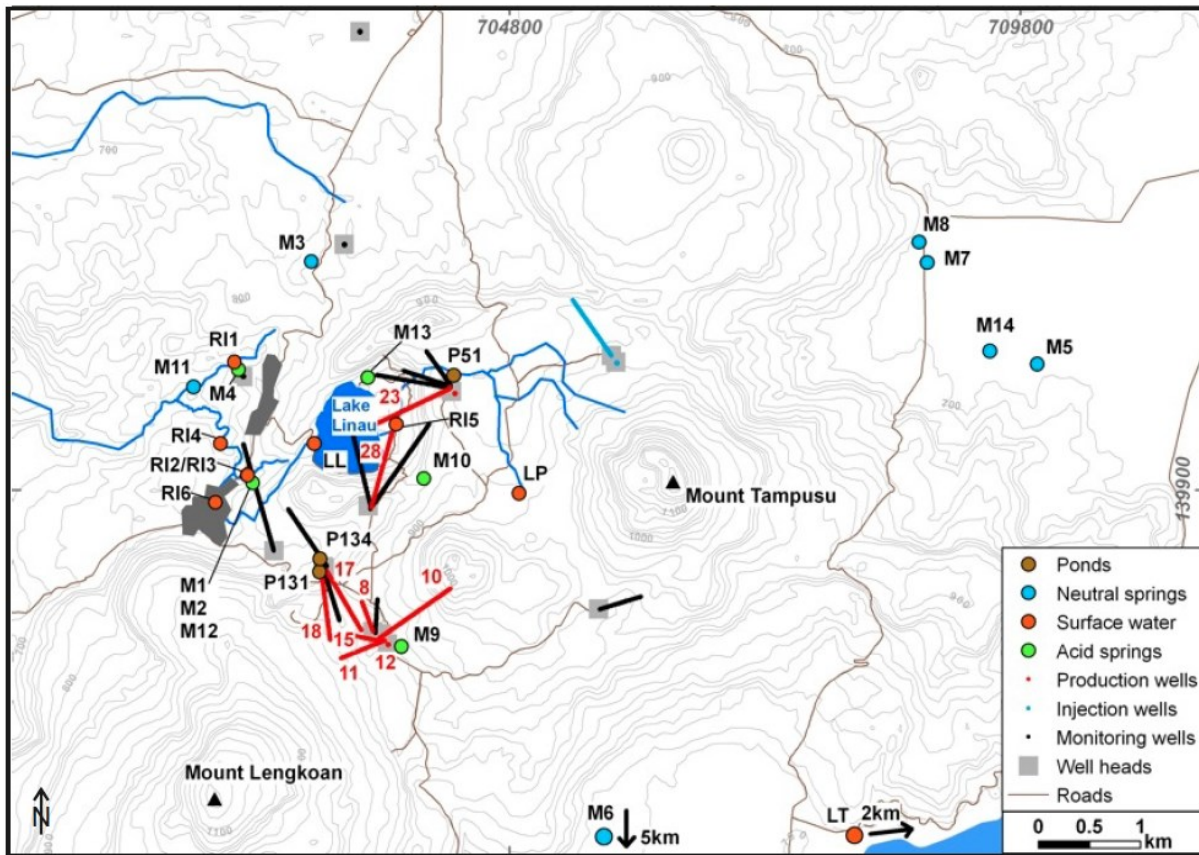


**Figure 1: Map of Lahendong geothermal field with sampling locations.**

North Sulawesi is formed by a volcanic arc and characterized by a complex geological history and tectonic regime in an arc-arc collision environment (Hamilton, 1979). The basement of North Sulawesi consists of a Cretaceous subduction complex (110 Ma) that is overlain by sedimentary and igneous sequences of Paleogene and Neogene age (Hamilton, 1979; Kavalieris et al., 1992). Two main pulses of magmatic activity (Early Miocene: 22-16 Ma and Late Miocene- to Quaternary: < 9 Ma) are related to pre- and post-collision events (Kavalieris et al., 1992 and references therein). Early Miocene arc assemblages are composed of calc-alkaline volcanic suites (mainly pyroxene andesite, pyroxene-hornblende andesite basalt, and co-magmatic I-type granitoids varying in composition between diorite and granite) and shallow marine sediments (andesitic greywacke and minor limestone). Magmatism of the Pliocene-Quaternary transition related to post-collisional rifting and uplift of the North Sulawesi arc include the large Tondano caldera. Within the Tondano caldera, several younger eruptions including the Linau volcano complex, the Tampusu complex, and the Pangolombian complex form the volcanic setting of Lahendong geothermal field (e.g., Poedjoprajitno, 2012).

According to Surachman et al. (1987), surface exposures of Quaternary volcanic rocks at Lahendong belong to the Post-Pangolombian Unit including the Linau sub-group (volcanic breccia, pyroclastic rocks, and andesitic lavas that form the Linau crater in the central part of Lahendong geothermal field, dated to  $0.46 \pm 0.04$  Ma (K-Ar), Utami et al., 2004), the Tampusu sub-group (basaltic andesite and pyroclastic rocks), and the Kasuratan sub-group (basaltic andesite lava). To the north, basaltic andesite of the Pre-Pangolombian Unit and to the south, andesitic and rhyolitic lavas of Mount Lengkoan are exposed (K-Ar:  $0.59 \pm 0.05$  Ma; Utami et al., 2004). Surface manifestations and hydrothermal alteration are associated with the local fault system and are mainly located in the surroundings of Lake Linau (e.g. Utami, 2011; Brehme et al., 2014).

Older subsurface lithological units (mainly identified from drill profiles in the Lahendong geothermal field) are divided into Pre-Tondano, Tondano, and Post-Tondano Units (e.g., Surachman et al., 1987; Utami et al., 2004; Koestono et al., 2010). The Post-Tondano Unit comprises volcanic rocks that were deposited after the formation of the volcano-tectonic Tondano depression. It consists of pyroclastic rocks and volcanic breccia, which are underlain by basaltic andesites (including lava flows from Pangolombian, Kasuratan, and Tampusu activity that are separated by thin paleo-soils). The Tondano Unit refers to volcanic rocks originating from the main stage of the Tondano eruption during the Pliocene/Early Pleistocene and is composed of rhyolitic-dacitic ignimbrites. The upper part of the formation contains abundant pumice, while the lower part is crosscut by micro-dioritic dyke intrusions. The Pre-Tondano Unit is composed of an alternating sequence of volcanic and sedimentary rocks that were deposited before the main Tondano eruption and are of Miocene to Pliocene age. Volcanic rocks include basaltic andesite, andesite, volcanic breccia, and pyroclastic rocks. Sedimentary rocks contain limestone and silty marl (Surachman et al., 1987).

### 3. METHODS

Fluid samples were collected from surface manifestations (hot springs), surface waters (streams, lakes), and deep production wells located between 1200 m and 1850 m below the surface in November 2011 (Fig. 1). All samples were filtered in the field ( $0.45 \mu\text{m}$  nylon filter) and stored in clean HDPE bottles prior to analysis.

For Sr isotope analysis, about 10 mL of the fluid samples were evaporated and dissolved in 1 mL of 2.5 N hydrochloric acid. Separation of Sr from other ions in the sample solution was carried out on ion-chromatography columns using Biorad AG 50x8 (200-400 mesh) resin and 2.5 N hydrochloric acid as eluent. Purified Sr fractions were loaded onto outgassed Re filaments (double-filament technique) with 0.25N H<sub>3</sub>PO<sub>4</sub> (ultrapure). Sr isotopes ratios were measured on a Finnigan MAT 262 thermal ionization mass spectrometer (TIMS) at the University of Goettingen, Germany. <sup>87</sup>Sr/<sup>86</sup>Sr ratios were corrected for instrumental fractionation using the natural <sup>88</sup>Sr/<sup>86</sup>Sr ratio of 8.375209. The analytical precision for the analyzed <sup>87</sup>Sr/<sup>86</sup>Sr ratios is 0.003% (2 $\sigma$ ) or less. Routine standard measurements yielded an average <sup>87</sup>Sr/<sup>86</sup>Sr ratio of 0.71039  $\pm$  0.00001 (2 $\sigma$ ; n=30) for the NBS987 Sr standard. Blanks for the chemical procedures were less than 0.5 ng for strontium.

For Ca isotope analysis, aliquots of the sample solutions were mixed with an appropriate amount of a <sup>42</sup>Ca-<sup>48</sup>Ca double spike of known isotopic composition in order to calculate for mass dependent fractionation during chemical sample preparation and mass spectrometric measurement (Skulan et al., 1997; Zhu et al., 1998). The sample-spike mixture was allowed to homogenize, and evaporated subsequently. The residue was dissolved in 2.5N HCl and loaded onto cation exchange columns using Biorad AG 50 x 8 resin. Purified Ca fractions were collected using 2.5N HCl and loaded onto outgassed Ta filaments with 0.25N H<sub>3</sub>PO<sub>4</sub> (ultrapure). Ca isotopes ratios were measured on a Finnigan MAT 262 thermal ionization mass spectrometer (TIMS) at the University of Goettingen, Germany. Ratios of <sup>40</sup>Ca, <sup>42</sup>Ca, <sup>44</sup>Ca, and <sup>48</sup>Ca were scanned at least 80 times per sample; replicates were run for selected samples. Routine standard measurements yielded an average <sup>44</sup>Ca/<sup>40</sup>Ca ratio of 0.021455  $\pm$  0.000003 (2 $\sigma$ ) (n=30) for seawater. Variations in the <sup>44</sup>Ca/<sup>40</sup>Ca are expressed in delta notation in ‰ relative to our measured seawater <sup>44</sup>Ca/<sup>40</sup>Ca ratio of 0.021455:

$$\delta^{44}\text{Ca} = \left( \frac{\frac{^{44}\text{Ca}}{^{40}\text{Ca}}_{\text{sample}}}{\frac{^{44}\text{Ca}}{^{40}\text{Ca}}_{\text{seawater}}} - 1 \right) \times 1000 \quad (1)$$

The analytical precision is 0.2 ‰ or less. Mass spectrometric analyses of the Ca reference standard NBS915b yielded an average  $\delta^{44}\text{Ca}$  value of  $-1.10 \pm 0.07$  ‰ (n=18) relative to seawater. Blanks for the chemical procedures are less than 1 ng for calcium. For isotopic analysis only distilled reagents were used.

## 4. RESULTS AND DISCUSSION

### 4.1 Hydrochemical characteristics of waters from Lahendong

The investigated water samples were grouped according to water type, pH range, and sampling location (for further details see Brehme et al., 2014).

#### 4.1.1 Group I

Group I comprises Na- and Ca-dominated bicarbonate waters (pH range: 5.8-8.1) from lakes, streams, shallow groundwater wells, and several hot springs. Lake and stream water shows generally lower concentrations in Na (3-20 mg/L), Ca (9-28 mg/L), Mg (4-8 mg/L), K (3-7 mg/L), and Si (<1-19 mg/L) compared to shallow groundwater (Na: 92-129 mg/L, Ca: 72-99 mg/L, Mg: 41-54 mg/L, K: 18-29 mg/L, and Si: 72-82 mg/L), and thermal waters from hot springs (Na: 19-98 mg/L, Ca: 11-78 mg/L, Mg: 5-40 mg/L, K: 6-17 mg/L, and Si: 60-93 mg/L).

#### 4.1.2 Group II

Group-II includes water from Lake Linau and hot springs located in the vicinity of the lake. The waters can be classified as Na- and Si-dominated acid-sulfate waters with pH values ranging between 2.0 and 2.7. Major cations show considerable variation: Na (2-159 mg/L), Si (58-148 mg/L), Ca (2-104 mg/L) Mg, and K are, 2-35 mg/L, and 5-17 mg/L, respectively.

#### 4.1.3 Group-III

Most of the deep production wells host Na- and Si-dominated chloride-type waters, while a few deep wells show Na- and Si-dominated bicarbonate-type composition. Na and Si concentrations of the chloride-type waters range from 87-853 mg/L and 127-364 mg/L, respectively, while Ca, Mg, and K show low concentrations (<6 mg Ca/L, <1 mg Mg/L, and 10-124 mg K/L) in those waters. For bicarbonate-type deep groundwater, concentrations of Na and Si range from 4-208 mg/L and 10-157 mg/L, respectively, with Ca, Mg, and K concentrations in similar ranges as for the chloride-type waters.

### 4.2 Sr isotopes

Sr isotopes are an indicator for the sources of dissolved Sr in natural waters, which are generally atmospheric inputs and weathering releases from minerals and rocks. Depending on the Sr concentration of the input sources and differences in weathering rates of the prevailing mineral phases, variation in the Sr isotope composition of natural waters reflect mixtures generated by the predominant Sr sources. In volcanic terrain, weathering of basaltic and andesitic rock usually produces distinctive isotopic compositions of dissolved Sr similar to the original bedrock. Variation in the Sr isotope composition of basaltic and andesitic rock reflected in groundwater may provide indications for hydrological pathways in the catchment and aquifer.

<sup>87</sup>Sr/<sup>86</sup>Sr ratios of the surface water, hot springs, and deep groundwater samples from Lahendong vary between 0.7039 and 0.7075 (Fig. 2). Water discharging at surface manifestations and from lakes and rivers generally have lower <sup>87</sup>Sr/<sup>86</sup>Sr ratios between 0.7039 and 0.7043, while deep groundwater shows higher values in the range of 0.7050 to 0.7075 with most samples plotting in a closer range between values of 0.7050 and 0.7053. The distinctive pattern of <sup>87</sup>Sr/<sup>86</sup>Sr ratios in waters discharging at the surface compared to groundwater from the deep reservoir suggests differences in the geochemical composition of the magmatic rocks forming the aquifer.

<sup>87</sup>Sr/<sup>86</sup>Sr ratios of Sangihe arc-related volcanic rocks from the Manado area (North Sulawesi) range between 0.7035 and 0.7048 (Elburg and Foden, 1998). Rock samples collected close to Lake Tondano (3 Ma) and from the Lokon (recent) vary from 0.7037 to

0.7039, and 0.7035 to 0.7038, respectively. Older (12-14 Ma) rocks in the area (e.g., from Ratatotok, which is located further south of Lake Tondano) show higher  $^{87}\text{Sr}/^{86}\text{Sr}$  ratios between 0.7039 and 0.7048 (Elburg and Foden, 1998). Similar results were reported by Tatsumi et al. (1991) for Tongkoko and Manado Tua lavas ( $^{87}\text{Sr}/^{86}\text{Sr}$ : 0.7036 to 0.7039). In contrast, igneous suites from west Sulawesi show generally higher  $^{87}\text{Sr}/^{86}\text{Sr}$  ratios between 0.710 and 0.722 indicating the involvement of continental crust in the subduction regime (Elburg and Foden, 1999), whereas magmatic rocks from northwest Sulawesi that are related to an oceanic arc setting have less-radiogenic  $^{87}\text{Sr}/^{86}\text{Sr}$  ratios between 0.7035 and 0.7074 (Elburg et al., 2003).

The good agreement between Sr isotope data of volcanic rocks exposed in the Manado/Tondano area (Tatsumi et al., 1991; Elburg and Foden, 1998) and the similarity in the range of  $^{87}\text{Sr}/^{86}\text{Sr}$  ratios of surface waters, shallow groundwater, and thermal water from most surface manifestations suggests an origin for Sr and other solutes in the younger and less altered volcanic rocks that are exposed on the surface or located in shallow depths as part of the Post-Tondano Unit. In turn, the higher  $^{87}\text{Sr}/^{86}\text{Sr}$  ratios of the deep thermal groundwaters collected in depths between about 1200 and 1850 m below the surface argues for an origin of dissolved Sr in andesitic rocks of the Pre-Tondano Unit that may be affected by crustal contamination as a source of radiogenic Sr. In addition, the high  $^{87}\text{Sr}/^{86}\text{Sr}$  ratio of 0.7075 analyzed for one of the deep wells may indicate the existence of a sedimentary Sr component in the reservoir fluids.

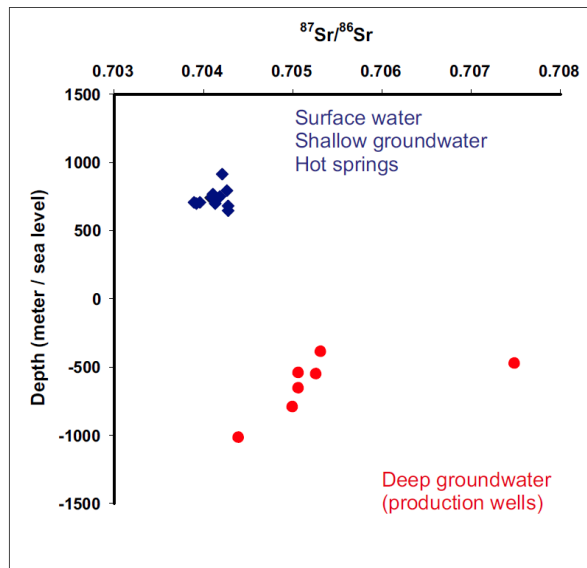


**Figure 2: Sr isotope distribution in water samples collected at Lahendong.**

Figure 2 displays a depth-related trend with increasing  $^{87}\text{Sr}/^{86}\text{Sr}$  ratios at decreasing depths for the groundwater samples from the deep production wells. This trend likely reflects crustal contamination of the mainly andesitic magmas at greater depths.

#### 4.3 Ca isotopes

$\delta^{44}\text{Ca}$  values of the water samples range from 0.09 to  $-1.52\text{ ‰}$ . The range of  $\delta^{44}\text{Ca}$  values is similar for both acid-sulfate waters (0.09 to  $-1.30\text{ ‰}$ ) and neutral waters from shallow and deep sources ( $-0.18$  to  $-1.52\text{ ‰}$ ).  $\delta^{44}\text{Ca}$  values do not correlate with  $^{87}\text{Sr}/^{86}\text{Sr}$  ratios suggesting that the distribution of Ca isotopes is not controlled by the sources of Ca but likely reflects dissolution/precipitation processes during the evolution of the thermal waters.

An average  $\delta^{44}\text{Ca}$  value of  $-0.97 \pm 0.19\text{ ‰}$  ( $n=10$ ) for various volcanic rocks was reported by Skulan et al. (1997). Provided that the  $\delta^{44}\text{Ca}$  value in the bulk rock is uniformly distributed, and fractionation of Ca isotopes is negligible during bedrock dissolution, the variation of  $\delta^{44}\text{Ca}$  values in the water is mainly affected by precipitation as well as mixing processes and potentially dissolution of secondary mineral phases. Experimental and field studies (under low-temperature conditions) suggest that precipitation of Ca-bearing mineral phases from aquatic solutions produces lower  $\delta^{44}\text{Ca}$  values in the precipitate and consequently higher  $\delta^{44}\text{Ca}$  values in the precipitating solution (e.g. Lemarchand et al., 2004). Therefore, it may be argued that low  $\delta^{44}\text{Ca}$  values in the water samples are associated with the dissolution of Ca-bearing mineral phases, and high  $\delta^{44}\text{Ca}$  values may be indicative for precipitation processes involving Ca-bearing secondary mineral phases.

Although we were not able to confirm the precipitation of calcium carbonate or sulfate from the hot springs, it is possible that Ca precipitates in conjunction with silicate mineral phases. We observed deposition of amorphous silica (confirmed by XRD analysis) at the hot springs. Parallel, Ca depletion from thermal water likely due to co-precipitation of Ca-phases with silica suggests fractionation of Ca isotopes. Accordingly, the negative correlation of  $\delta^{44}\text{Ca}$  values and Ca/Si ratios ( $R^2=0.67$ ) may be regarded as an indicator for precipitation/dissolution processes, where high Ca/Si ratios parallel to low  $\delta^{44}\text{Ca}$  values suggest dissolution of mineral phases, and low Ca/Si ratios parallel to high  $\delta^{44}\text{Ca}$  values suggest depletion of Ca from solution by co-precipitation of Ca- and Si-phases (Fig. 3a).

For the deep groundwater wells, similar negative trends exist for  $\delta^{44}\text{Ca}$  values and Ca/Si ratios (Fig. 3b). Those trends could likewise be indicative for complex precipitation/dissolution processes including secondary Ca-bearing carbonate or sulfate minerals in the reservoir.

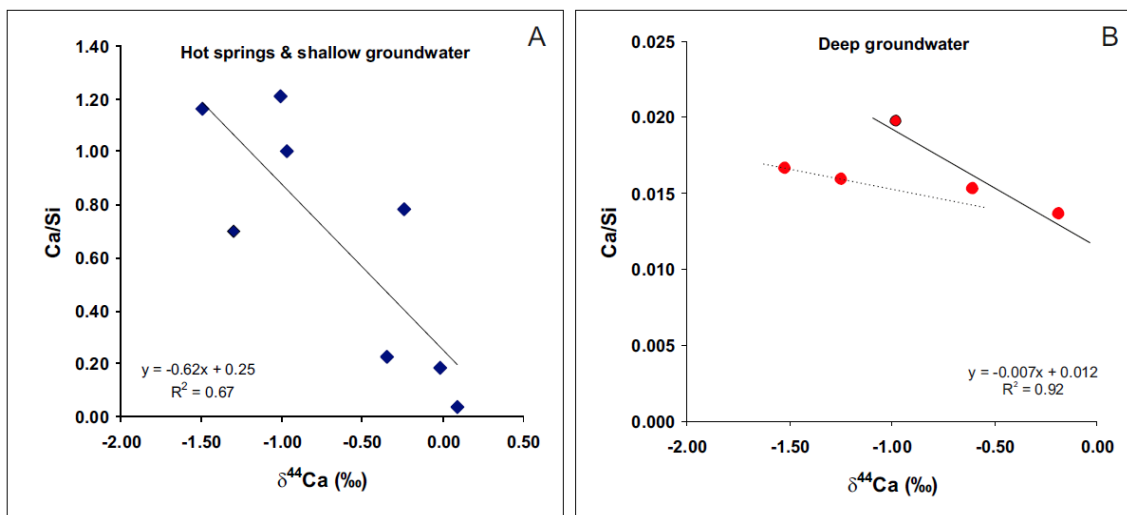


**Figure 3: Distribution of  $\delta^{44}\text{Ca}$  values and Ca/Si ratios in (a) hot springs and shallow groundwater and (b) deep groundwater from production wells.**

Utami (2011) identified calcite, epidote, and gypsum/anhydrite as replacements for plagioclase and pyroxene or as direct deposits in fractures and cavities. Low  $\delta^{44}\text{Ca}$  values in conjunction with elevated Ca/Si ratios suggest dissolution of secondary mineral deposits, while higher  $\delta^{44}\text{Ca}$  values may indicate precipitation of Ca-bearing phases in the reservoir. Ca and Si concentrations are significantly correlated for the deep wells ( $R^2=0.94$ ), whereas for the hot springs and shallow groundwater wells a correlation between the two elements is lacking. In addition, Ca/Si ratios are significantly lower (0.014 to 0.017) in the reservoir compared to groundwater from the shallow aquifer and thermal springs (0.18 to 1.21) as a result of the strong depletion of Ca from the hydrothermally altered deep reservoir rocks in contrast to the younger and less weathered rocks exposed at the surface.

## 5. CONCLUSION

Based on geochemical and Sr isotope characteristics, two main sources of solutes can be distinguished: a) solutes that are generated in young lava flows which constitute the shallow aquifer (solute are mainly derived from weathering of primary minerals like plagioclase and pyroxenes) and b) solutes generated in highly weathered and hydrothermally altered magmatic rocks of the deep reservoir.

Surface water, shallow groundwater and hot springs show elevated concentrations of Ca, Mg, and Sr, and low Sr isotope ratios that are characteristic for weathering-releases associated with young and little weathered lava flows, while for the deep aquifer system, geothermal waters are considerably depleted in those elements but show elevated Si concentrations due to the strong alteration of the bedrock. In addition, the higher  $^{87}\text{Sr}/^{86}\text{Sr}$  ratio of the deep groundwater differs significantly from the lower  $^{87}\text{Sr}/^{86}\text{Sr}$  ratio analyzed for waters associated with the shallow aquifer system. The more radiogenic Sr isotope composition of the deep groundwater is caused by compositional differences in the geochemistry of the reservoir rocks as a result of crustal contamination and/or minor intercalation of sedimentary rocks. The distribution of Ca isotopes in the water samples suggests complex dissolution/precipitation processes in both the shallow and the deep aquifer.

**Acknowledgement:** The authors would like to thank the team of Pertamina Geothermal Energy in Lahendong and Jakarta for their permission and support during the sampling campaign. This research was funded by the German Federal Ministry for Education and Research (BMBF) as part of the project “Sustainability concepts for exploitation of geothermal reservoirs in Indonesia – capacity building and methodologies for site deployment” (Grant 03G0753A).

## REFERENCES

Aquilina, L., Pauwels, H., Genter, A., and Fouillac, C.: Water-rock interaction processes in the Triassic sandstone and the granitic basement of the Rhine Graben: Geochemical investigation of a geothermal reservoir. *Geochim. Cosmochim. Acta*, **61**, (1997), 4281-4295.

Brehme, M., Moeck, I., Kamah, Y., Zimmermann, G., and Sauter, M.: A hydrogeological model of a geothermal reservoir – A study in Lahendong, Indonesia. *Geothermics*, **51**, (2014), 228-239.

Brown, S.T., Kennedy, B.M., DePaolo, D.J., Hurwitz, S., and Evans W.C.: Ca, Sr, O and D isotope approach to defining the chemical evolution of hydrothermal fluids: Example from Long Valley, CA, USA. *Geochim. Cosmochim. Acta*, **122**, (2013), 209-225.

Bullen, T.D., Krabbenhoft, D.P., and Kendall, C.: Kinetic and mineralogic controls on the evolution of groundwater chemistry and  $^{87}\text{Sr}/^{86}\text{Sr}$  in a sandy silicate aquifer, northern Wisconsin. *Geochim. Cosmochim. Acta*, **60**, (1996), 1807–1821.

Druhan, J.L., Steefel, C.I., Williams, K.H., and DePaolo, D.J.: Calcium isotope fractionation in groundwater: Molecular scale processes influencing field scale behavior. *Geochim. Cosmochim. Acta*, **119**, (2013), 93–116.

Elburg, M., and Foden, J.: Sources for magmatism in Central Sulawesi: Geochemical and Sr-Nd-Pb constraints. *Chem. Geol.*, **156**, (1999), 67–93.

Elburg, M., van Leeuwen, T., Foden, J., and Muhardjo: Spatial and temporal isotopic domains of contrasting igneous suites in Western and Northern Sulawesi, Indonesia. *Chem. Geol.*, **199**, (2003), 243– 276.

Elburg, M.A., and Foden, J.D.: Temporal changes in arc magma geochemistry, north Sulawesi, Indonesia. *Earth Planet. Sci. Lett.*, **163**, (1998), 381-398.

Elderfield, H. and Greaves, M.J.: Strontium isotope geochemistry of Icelandic geothermal systems and implications for seawater chemistry. *Geochim. Cosmochim.*, **45**, (1981), 221-2212.

Graham, I.J.: Strontium isotope composition of Rotorua Geothermal Waters. *Geothermics*, **21**, (1992), 165-180.

Grimes, S., Rickard, D., Hawkesworth, C., van Calsteren, P., and Browne, P.: The Broadlands–Ohaaki geothermal system, New Zealand Part 1. Strontium isotope distribution in well BrO-29. *Chem. Geol.*, **163**, (2000), 247–265.

Grobe, M., Machel, H.G., and Heuser, H.: Origin and evolution of saline groundwater in the Münsterland Cretaceous Basin, Germany: oxygen, hydrogen, and strontium isotope evidence. *J. Geochem. Explor.*, **69–70**, (2000), 5–9.

Hamilton, W.: Tectonics of the Indonesian Region, *Geol. Surv. Prof. Pap.* **1078**, 345 pp. (1979).

Jacobson, A.D., and Holmden, C.:  $\delta^{44}\text{Ca}$  evolution in a carbonate aquifer and its bearing on the equilibrium isotope fractionation factor for calcite. *Earth Planet. Sci. Lett.*, **270**, (2008), 349–353.

Kavalieris, I., van Leeuwen, TH.M., and Wilson, M.: Geological setting and styles of mineralization, north arm of Sulawesi, Indonesia. *J. Southeast Asian Earth Sci.*, **7**, (1992), 113-129.

Koestono, H., Siahaan, E.E., Silaban, M., and Franzson, H.: Geothermal Model of the Lahendong Geothermal Field, Indonesia. *Proceedings World Geothermal Congress 2010*, Bali, Indonesia, (2010).

Lemarchand, D., Wasserburg, G.J., and Papanastassiou, D.A.: Rate-controlled calcium isotope fractionation in synthetic calcite. *Geochim. Cosmochim. Acta*, **68**, (2004), 4065-4678.

McNutt, R.H., Frape, S.K., and Dollar, P.: A strontium, oxygen and hydrogen isotopic composition of brines, Michigan and Appalachian Basins, Ontario and Michigan. *Appl. Geochem.*, **2**, (1987), 495–505.

Millot, R., Hegan, A., and Négrel, P.: Geothermal waters from the Taupo Volcanic Zone, New Zealand: Li, B and Sr isotopes characterization. *Applied Geochem.*, **27**, (2012), 677–688.

Millot, R., and Négrel, P.: Multi-isotopic tracing ( $\delta^7\text{Li}$ ,  $\delta^{11}\text{B}$ ,  $\delta^{87}\text{Sr}/\delta^{86}\text{Sr}$ ) and chemical geothermometry: evidence from hydro-geothermal systems in France. *Chem. Geol.*, **244**, (2007), 664–678.

Nielsen, L.C., and DePaolo, D.J.: Ca isotope fractionation in a high-alkalinity lake system: Mono Lake, California. *Geochim. Cosmochim. Acta*, **118**, (2013), 276–294.

Poedjoprajitno, S.: Morphostructure Control Towards the Development of Mahawu Volcanic Complex, North Sulawesi. *Indonesian Journal of Geology*, **7**, (2012), 39-54.

Skulan J., DePaolo D.J., and Owens, T.L.: Biological control of calcium isotopic abundances in the global calcium cycle. *Geochim. Cosmochim. Acta*, **61**, (1997), 2505–2510.

Surachman, S., Tandirerung, S.A., Buntaran, T., and Robert, D.: Assessment of the Lahendong Geothermal Field, North Sulawesi, Indonesia. *Proceeding Indonesian Petroleum Association, 16th Annual Convention*, (1987), 385-398.

Tang J.W., Dietzel M., Böhm F., Köhler S.J., and Eisenhauer A.:  $\text{Sr}^{2+}/\text{Ca}^{2+}$  and  $^{44}\text{Ca}/^{40}\text{Ca}$  fractionation during inorganic calcite formation: II. Ca isotopes. *Geochim. Cosmochim. Acta*, **72**, (2008), 3733–3745.

Tatsumi, Y., Murasaki, M., Arsade, E.M., and Nohda, S.: Geochemistry of Quaternary lavas from NE Sulawesi: transfer of subduction components into the mantle wedge. *Contrib. Mineral. Petrol.*, **107**, (1991), 137–149.

Tipper, E.T., Galy, A., and Bickle, M.J.: Calcium and magnesium isotope systematics in rivers draining the Himalaya-Tibetan-Plateau region: Lithological or fractionation control? *Geochim. Cosmochim. Acta*, **72**, (2008), 1057–1075.

Utami, P.: Hydrothermal alteration and the evolution of the Lahendong geothermal system, North Sulawesi, Indonesia. *Doctoral thesis*, University of Auckland, New Zealand, 449 p. (2011).

Utami, P., Siahaan, E.E., Azimudin, T., Suroto, Browne, P.R.L., and Simmons, S.F.: Overview of the Lahendong geothermal field, North Sulawesi, Indonesia: a progress report. *Proceedings 26th NZ Geothermal Workshop 2004*, (2004), 6-11.

Wiegand, B.: Tracing effects of decalcification on solute sources in a shallow groundwater aquifer, NW Germany. *Journal of Hydrology*, **378**, (2009), 61-72.

Wiegand, B., Dietzel, M., Bielert, U., Groth, P., and Hansen, B.T.:  $^{87}\text{Sr}/^{86}\text{Sr}$ -Verhältnisse als Tracer für geochemische Prozesse in einem Lockergesteinsaquifer (Liebenau, NW-Deutschland). *Acta Hydrochim. Hydrobiol.*, **29**, (2001), 139–152.

Wiegand, B.A., and Schwendenmann, L.: Determination of Sr and Ca sources in small tropical catchments (La Selva, Costa Rica) – A comparison of Sr and Ca isotopes. *Journal of Hydrology*, **488**, (2013), 110–117.

Wiegand, B.A., Dietzel, M., Leis, A., Benischke, R., and Haensel, S.: Evolution of  $\delta^{13}\text{C}$  and  $\delta^{44}\text{Ca}$  in calcite and spring water (Carinthia, Austria). *Geophys. Research Abstracts*, Vol. **8**, 09890 (2006).

Zhu P. and Macdougall D.: Calcium isotopes in the marine environment and the oceanic calcium cycle. *Geochim. Cosmochim. Acta*, **62**, (1998), 1691–1698.